Development 137, 3857-3866 (2010) doi:10.1242/dev.054866

The CRL2^{LRR-1} ubiquitin ligase regulates cell cycle progression during *C. elegans* development

Jorge Merlet*, Julien Burger*, Nicolas Tavernier, Bénédicte Richaudeau, José-Eduardo Gomes and Lionel Pintard†

SUMMARY

The molecular mechanisms that regulate cell cycle progression in a developmental context are poorly understood. Here, we show that the leucine-rich repeat protein LRR-1 promotes cell cycle progression during *C. elegans* development, both in the germ line and in the early embryo. Our results indicate that LRR-1 acts as a nuclear substrate-recognition subunit of a Cullin 2-RING E3 ligase complex (CRL2^{LRR-1}), which ensures DNA replication integrity. LRR-1 contains a typical BC/Cul-2 box and binds CRL2 components in vitro and in vivo in a BC/Cul-2 box-dependent manner. Loss of *lrr-1* function causes cell cycle arrest in the mitotic region of the germ line, resulting in sterility due to the depletion of germ cells. Inactivation of the DNA replication checkpoint signaling components ATL-1 and CHK-1 suppresses this cell cycle arrest and, remarkably, restores *lrr-1* mutant fertility. Likewise, in the early embryo, loss of *lrr-1* function induces CHK-1 phosphorylation and a severe cell cycle delay in P lineage division, causing embryonic lethality. Checkpoint activation is not constitutive in *lrr-1* mutants but is induced by DNA damage, which may arise due to re-replication of some regions of the genome as evidenced by the accumulation of single-stranded DNA-replication protein A (ssDNA-RPA-1) nuclear foci and the increase in germ cell ploidy in *lrr-1* and *lrr-1; atl-1* double mutants, respectively. Collectively, these observations highlight a crucial function of the CRL2^{LRR-1} complex in genome stability via maintenance of DNA replication integrity during *C. elegans* development.

KEY WORDS: E3 ubiquitin ligase, DNA replication, Checkpoint, Cell cycle, ATR/ATL-1, Chk1/CHK-1, *Caenorhabditis elegans*

INTRODUCTION

DNA replication is a period of extreme vulnerability for the genome of eukaryotic cells. During this complex process replication forks frequently encounter obstacles that impede their progression. Stalled forks are unstable structures that have to be stabilized and restarted in order to achieve faithful duplication of the genome. To cope with stalled replication forks and other forms of DNA damage, cells have evolved surveillance mechanisms, termed DNA damage and replication checkpoints, that scrutinize DNA damage and replication stress and orchestrate the appropriate cellular responses (Harper and Elledge, 2007; Paulsen and Cimprich, 2007). These signaling cascades are initiated by loading and activation of the PI3 kinase-related kinase ataxia telengectasia and Rad3 related (ATR) at sites of damage (Cimprich and Cortez, 2008). Once recruited to the stalled replication fork, ATR phosphorylates and thereby activates Chk1, which in turn blocks cell cycle progression, prevents origin firing, stabilizes stalled replication forks and facilitates the restart of collapsed forks.

The ATR/Chk1 signaling pathway is also mobilized during development to control cell cycle duration. For example, in the *C. elegans* embryo, this pathway is specifically activated by developmental cues to control cell cycle timing (Brauchle et al., 2003). This checkpoint is preferentially activated in the P lineage, or future germ line of the animal, such that at the two-cell stage the P1 blastomere invariably enters mitosis 2 minutes after the anterior AB blastomere (Brauchle et al., 2003; Moser et al., 2009). This asynchrony of cell division is crucial for germ line and embryonic development, as shortening the delay through inactivation of the ATL-1/CHK-1 (the *C. elegans* orthologs of ATR/Chk1) pathway leads to sterility, whereas lengthening the cell cycle through hyperactivation of this pathway causes patterning defects and embryonic lethality (Encalada et al., 2000; Brauchle et al., 2003; Kalogeropoulos et al., 2004; Holway et al., 2006). Therefore, activation of the ATL-1/CHK-1 pathway by DNA damage is actively suppressed in early embryos so that P lineage cell divisions occur on schedule (Holway et al., 2006). DNA damage resulting from severe DNA replication defects does eventually delay cell cycle progression in a checkpoint-dependent manner and the P1 blastomere is affected more strongly by this delay than the AB blastomere (Brauchle et al., 2003).

In sharp contrast to the early embryo, in which the fast pace of development is favored at the expense of genome stability, germ cells are highly sensitive to genotoxic insults and replication stress (Gartner et al., 2000). Under these conditions, the ATL-1/CHK-1 pathway is required to transiently arrest cell cycle progression (Garcia-Muse and Boulton, 2005), presumably to allow time for DNA repair. This cell cycle arrest causes a severe reduction in the number of germ cell nuclei, which become enlarged because nuclear and cellular growth continue during the arrest (Gartner et al., 2000).

In this study, we report that leucine-rich repeat protein 1 (LRR-1) is an essential determinant of genome stability in *C. elegans* and acts as a substrate-recognition subunit of a Cullin 2-RING E3 ligase complex (CRL2^{LRR-1}). LRR-1 is a nuclear protein that contains a typical BC/Cul-2 box, which is the signature of CRL2 substrate-recognition subunits, and binds CRL2 components

Institut Jacques Monod, CNRS, Université Paris Diderot, Bâtiment Buffon 15 rue Hélène Brion, 75205 Paris cedex 13, France.

*These authors contributed equally to this work
†Author for correspondence (pintard.lionel@ijm.univ-paris-diderot.fr)

Accepted 16 September 2010

through this motif both in vitro and in vivo. Although *lrr-1* is an essential gene, maternal rescue allows the analysis of *lrr-1* loss of function in adult tissues. *lrr-1* mutants are sterile owing to severe defects in germ cell proliferation. Inactivation of ATL-1/CHK-1 checkpoint components suppresses this proliferation defect and, remarkably, fully restores *lrr-1* mutant fertility. Likewise, in the early embryo, *lrr-1* inactivation leads to hyperactivation of the ATL-1/CHK-1 pathway, which delays mitotic entry and results in embryonic lethality. Checkpoint activation is not constitutive in *lrr-1* mutants but is induced by DNA damage, which may arise due to DNA re-replication problems.

MATERIALS AND METHODS

Nematode strains, strain construction and culture conditions

C. elegans strains were cultured and maintained using standard procedures (Brenner, 1974). The *lrr-1(tm3543)* allele was generated and kindly provided by S. Mitani of the National BioResource Project for the nematode, Japan. Deletions were backcrossed four times with the wild-type N2 strain (Bristol) and then balanced with the balancer chromosome mIn1 (Edgley and Riddle, 2001). Strains of the following genotypes were used: *lrr-1(tm3543); leals30[unc-119(+) pie-1::GFP::lrr-1]* (this study); XA3501: *unc-119(ed3); ruIs32[unc-119(+) pie-1::GFP::his11] III*; *ojIs1[unc-119(+) pie-1::GFP::tbb-2]*; *div-1(or148ts)* (Encalada et al., 2000); and *atl-1(tm853) IV/nT1[qIs50]* (IV;V) (Garcia-Muse and Boulton, 2005).

RNA-mediated interference (RNAi)

RNAi was performed by the feeding method (Kamath et al., 2001). RNAi-depleted embryos that were able to divide at least until the four-cell stage were analyzed. For strains expressing fluorescent proteins, RNAi was performed at 20°C or 25°C.

Hydroxyurea (HU) treatment

L1 larvae were grown until adulthood on NGM plates containing HU (6 and 8 mM) at 20°C. Animals were then paralyzed with levamisole (20 mM; Sigma) and examined under a Zeiss Axioimager A1 microscope equipped with DIC optics.

DNA manipulation and worm injection

Molecular biology was performed using standard procedures (Sambrook et al., 1989). The polycistronic vector pST39 was obtained from S. Tan (Tan, 2001). The fosmid WRM0634DD04 containing the *lrr-1* gene was obtained from Geneservice and prepared according to the manufacturer's instructions. WRM0634DD04 (20 ng/μl) was injected into *lrr-1(tm3543)* heterozygous animals together with pRF4 (80 ng/μl) containing the *rol-6(D)(su1006)* mutant gene (Mello et al., 1991) and *myo-2::RFP* (50 ng/μl) as a co-injection marker, giving a total concentration of 150 μg/ml per injection.

Antibodies, protein extracts and immunopurification

LRR-1, CUL-2 and ELC-1 proteins were expressed as fusions with glutathione-S-transferase (GST) in *E. coli* BL21, purified from inclusion bodies and used to immunize rabbits (Charles River Laboratories). The generated antibodies were affinity purified on nitrocellulose strips as described previously (Pintard et al., 2003). The antibodies used in this study included FLAG (1/1000; Sigma), T7 (1/6000; Novagen), Mab414 (1/500; Covance), phospho-serine histone H3 (1/100; Cell Signaling), phospho-Y15 CDK-1 (Calbiochem), phospho-S345 CHK-1 (Abcam), CDC-25.1 (Segref et al., 2010), RPA-1 (Lee et al., 2010), GFP (1/1000; Roche), mouse TrueBlot horseradish peroxidase (1/1000; eBioscience), ELC-1 (1/500; this study), CUL-2 (1/500; this study) and LRR-1 [1/50 (immunofluorescence) and 1/500 (western blot); this study].

Protein extraction and immunoprecipitation experiments were performed as previously described (Luke-Glaser et al., 2007). The expression of recombinant proteins was induced by the addition of 1 mM isopropyl β-D-thiogalactopyranoside to 1-liter cultures of *E. coli* BL21 before incubation overnight at 18°C. After pelleting, the bacteria were resuspended in 20 ml 0.15 M NaCl, 0.5 mM dithiothreitol, 40 mM imidazole in PBS, pH 7.3, before lysis using an Emulsiflex homogenizer (Avestin). The soluble portion of the lysate was loaded on a 1-ml Hi-Trap HP Column (GE Healthcare). The column was washed with ten volumes of lysis buffer, and bound proteins were eluted in lysis buffer containing 300 mM imidazole.

HEK293T cell culture and transfection

Human embryonic kidney HEK293T cells were cultured as described (Luke-Glaser et al., 2007). Six hours before immunopurification, the proteasome inhibitor MG132 (20 μM) was added to the culture.

Immunostaining, live imaging and fluorescence microscopy

The gonads were dissected by opening the worms in PBS buffer behind the pharyngeal bulb. Worms and embryos were freeze-cracked by flipping off the coverslip, immobilized on poly-lysine-coated slides and fixed for 20 minutes in methanol at –20°C. Affinity-purified LRR-1 antibody was used at a dilution of 1:50 and the secondary antibodies were coupled to the fluorophores Alexa 488 or Alexa 543 (Molecular Probes) and used at 1:400. Embryos were mounted in Vectashield Mounting Medium with DAPI (Vector). To determine cell cycle length, early embryo divisions were recorded at 20°C by taking images at 10-second intervals using a 63× objective on a DMI 6000 microscope (Leica) equipped with DIC optics and a high-resolution CoolSNAP HQ2 camera (Photometrics) driven by MetaMorph 7 software (Universal Imaging). Fixed germ lines and embryos were imaged on a DM IRB inverted microscope (Leica), a CSU-10 spinning Nipkow disk confocal unit (Yokogawa Electric, Tokyo, Japan) equipped with a CoolSNAP HQ camera (Fig. 2A), a TCS SP5 confocal microscope (Leica) (Fig. 3C, Fig. 5 and Fig. 6C) or an Axiovert 200 inverted microscope (Zeiss) equipped with the ApoTome module (Zeiss) (Fig. 2B).

Propidium iodide staining and genomic DNA quantification

Wild-type and *lrr-1(tm3543)* mutant germ lines were dissected on the same slide 24 hours post L4 stage, permeabilized and fixed as described above. After RNase A treatment, germ cells were stained with propidium iodide (40 μg/ml). Slides were mounted and *z*-stacks were imaged at 0.3 μM with a 63× objective on an SP2 confocal microscope (Leica) at maximum resolution, using the same parameters for each slide. We then reconstructed each germ line in three dimensions using Imaris v5.5 software (Bitplane). To determine the quantity of genomic DNA per germ cell nucleus, we quantified the fluorescence of each pixel contained within the volume of the nucleus. To define a 2N- and 4N-equivalent amount of genomic DNA, we used germ cell nuclei in anaphase as a reference, in which each mass of DNA was assumed to have a 2N DNA content. The nuclei contained in the mitotic region were classified according to their DNA content (2N, 2N<X<4N, 4N or >4N).

RESULTS

LRR-1 (F33G12.4) is a substrate-recognition subunit of a CRL2 complex in *C. elegans*

Cullin-RING E3 ligases (CRLs) are multisubunit enzymes that comprise cullin-based catalytic cores and exchangeable substrate-recognition modules, which selectively recruit substrates for ubiquitylation by an associated E2 enzyme (Petroski and Deshaies, 2005). In Cullin 2-based ubiquitin ligases (CRL2), the substrate-recognition module comprises the adaptor protein Elongin C (ELC-1), which, along with Elongin B (ELB-1), bridges the interaction between the N-terminal part of Cullin 2 (CUL-2) and the BC/Cul-2 box-containing protein that selectively recruits substrates (Fig. 1A). The BC/Cul-2 box includes two short sequences, termed BC and the Cul-2 box, that are required for ELC-1 and CUL-2 binding, respectively (Vasudevan et al., 2007; Mahrour et al., 2008). Through proteomic screens in mammalian cells (HEK293T), we and others have identified LRR-1 as a potential substrate-recognition subunit of a CRL2 complex (Kamura et al., 2004; Olma et al., 2009). Although LRR-1 is evolutionarily conserved, its function remains elusive.

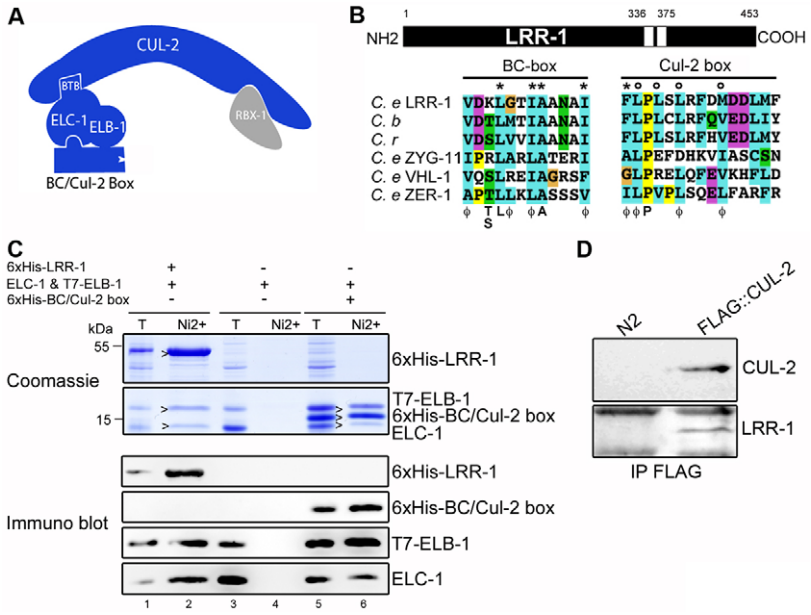

Fig. 1. LRR-1 (F33G12.4) binds CRL2 components in vitro and in vivo in a BC/Cul-2 box-dependent manner. (**A**) The CRL2 complex, in which the BC/Cul-2 box protein functions as a substrate-recognition subunit. BTB, Bric a brac, Tramtrack, Broad complex. (**B**) (Above) Domain organization of LRR-1. (Below) Alignment of the BC/Cul-2 box sequences of LRR-1 from various nematode species (*C. e*, *C. elegans*; *C. b*, *C. briggsae*; *C. r*, *C. remanei*) and *C. elegans* ZYG-11, VHL-1 and ZER-1. Conserved amino acids are highlighted: P, yellow; G, orange; S/T/Q/N, green; E/D, purple; W/L/V/I/M/A/F/C/Y/H, blue. A consensus is provided below the alignment; ϕ, aliphatic amino acids. Residues in BC/Cul-2 box sequences that make contact with ELC-1 (*) and CUL-2 (°) are shown above the alignment. (**C**) The indicated proteins were co-expressed in *E. coli* from a polycistronic vector (+, expressed; –, not expressed), affinity purified on Hi-TRAP columns charged with Ni^{2+} ions and analyzed by SDS-PAGE. The gel was either stained with Coomassie Brilliant Blue (upper panels) or immunoblotted with His, T7 or ELC-1 antibodies (lower panels). T, total extracts (lanes 1, 3 and 5); Ni^{2+}, eluates (lanes 2, 4 and 6). Arrowheads mark the positions of the purified proteins. (**D**) Total protein extracts from wild-type N2 animals or those expressing FLAG::CUL-2 were incubated with anti-FLAG (M2) agarose beads. The immunoprecipitates were separated by SDS-PAGE and immunoblotted with CUL-2 (top) or LRR-1 (bottom) antibodies.

The *C. elegans* genome encodes one open reading frame with similarities to human LRR-1 (PPIL5 – Human Genome Nomenclature Committee) (Flicek et al., 2010). The uncharacterized F33G12.4 protein (henceforth called LRR-1) has a similar organization and, like its human counterpart, contains several leucine-rich repeats (LRRs) followed at the C-terminus by a putative BC/Cul-2 box (residues 336-375) (Fig. 1B). Multiple sequence alignment of LRR-1 with selected BC/Cul-2 box-containing proteins from *C. elegans* revealed that these two motifs are conserved in LRR-1. In particular, the key residues that mediate binding to ELC-1 and CUL-2 (Stebbins et al., 1999; Vasudevan et al., 2007; Mahrour et al., 2008) are invariant in LRR-1 (Fig. 1B), suggesting that it is a bona fide substrate-recruitment subunit of a CRL2 complex in *C. elegans*.

To test this hypothesis, we expressed LRR-1 in *E. coli* and performed in vitro binding experiments with CRL2 components. The LRR-1 polypeptide, however, failed to fold properly in bacteria and was consistently recovered in the insoluble fraction of the cell extract (data not shown). To circumvent this problem, we co-expressed 6×His-tagged LRR-1 together with ELC-1 and ELB-1 from a polycistronic vector (see Materials and methods). Under these conditions, 6×His-LRR-1 was readily recovered in the soluble fraction of the bacterial extract and was retained on nickel beads in a complex containing ELB-1 and ELC-1 (Fig. 1C, lane 2), whereas neither ELB-1 nor ELC-1 was retained on nickel beads in the absence of LRR-1 (Fig. 1C, lane 4). Importantly, the domain encompassing the LRR-1 BC/Cul-2 box (residues 278-399) was sufficient to co-purify ELC-1 and ELB-1 (Fig. 1C, lane 6). LRR-1 also bound CRL2 components in vivo, as shown by its specific co-precipitation from total worm extracts with a FLAG-tagged version of CUL-2 (Fig. 1D).

C. elegans LRR-1 therefore has the hallmarks of a substrate-recognition subunit of a CRL2 complex: (1) the presence of a BC/Cul-2 box and an additional protein-protein interaction domain (LRRs); (2) a physical interaction with ELC-1 and ELB-1 in a BC/Cul-2 box-dependent manner; and (3) an association with CUL-2 in vivo.

LRR-1 is a nuclear protein and its localization depends on CUL-2 and ELB-1

Next, we analyzed the subcellular localization of LRR-1 by immunofluorescence using specific antibodies (Fig. 2). Given that *lrr-1* mRNA is germ line enriched (Reinke et al., 2000), we examined LRR-1 protein levels and localization in the adult germ line and in early embryos. The *C. elegans* germ line consists of two ‘U-shaped’ tubes, each of which contains a syncitium of hundreds of nuclei subdivided into a mitotic zone and a meiotic zone (Fig. 2A) (Kimble and Crittenden, 2007). The mitotic zone is located at the distal end of each tube and contains the mitotic germ cells, which serve as transient amplifying cells (Kimble and White, 1981). As germ nuclei move proximally, they exit the mitotic cycle to enter meiosis. As shown in Fig. 2A, LRR-1 was present throughout the germ line in both the mitotic and meiotic zones, where it localized to the nucleus, but it appeared to be excluded from the chromosomes as no co-staining with DAPI could be detected. In early embryos, LRR-1 was also enriched in the

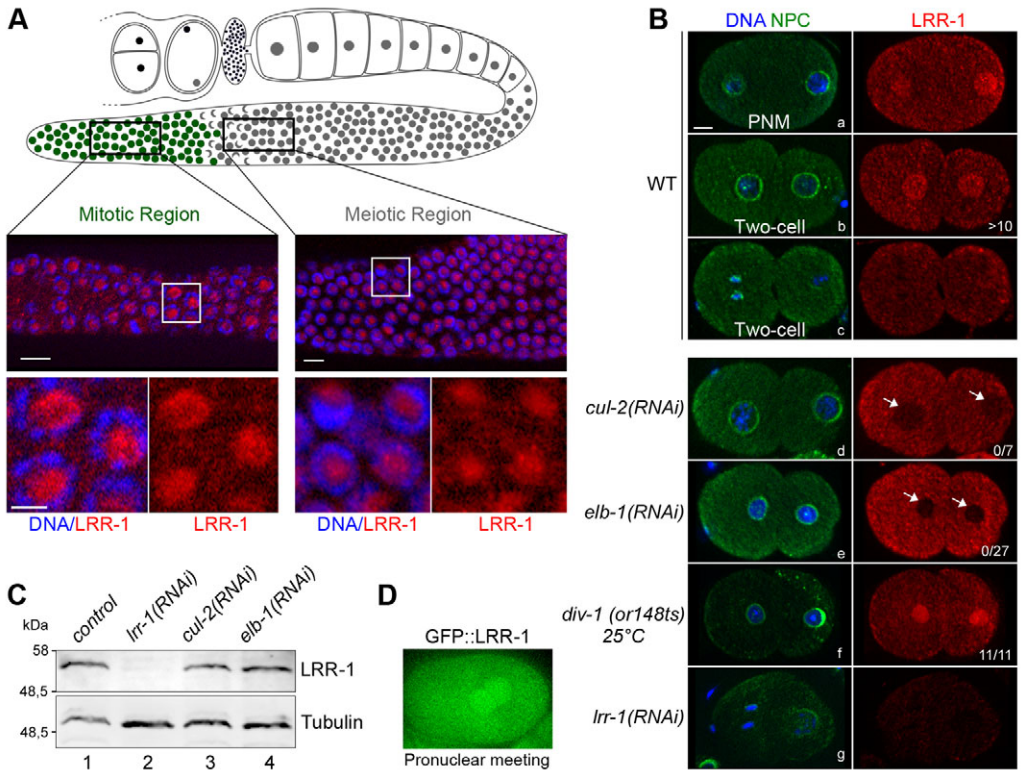

Fig. 2. LRR-1 is nuclear in germ cells and in the early embryo and its nuclear localization depends on ELB-1 and CUL-2. (**A**) (Above) Diagram of one arm of the adult *C. elegans* hermaphrodite gonad. (Below) Representative images of fixed wild-type N2 germ lines stained with LRR-1 antibodies (red) and counterstained with DAPI (blue). Scale bars: 20 μm. The boxed regions, encompassing representative nuclei from the mitotic and meiotic regions of the gonad, are shown at higher magnification beneath. Scale bar: 5 μm. (**B**) Fixed (**a**,**b**,**c**) wild-type, (**d**) *cul-2(RNAi)*, (**e**) *elb-1(RNAi)*, (**f**) *div-1(or148ts)* and (**g**) *lrr-1(RNAi)* embryos stained with LRR-1 (red) and nucleoporin/Mab414 (green) antibodies and counterstained with DAPI (blue). The fraction of embryos that showed the wild-type LRR-1 staining is indicated at the bottom right of each image. The nuclear localization of LRR-1 was abrogated in *cul-2* and *elb-1(RNAi)* embryos (arrows). Anterior is to the left in this and other figures. Scale bar: 5 μm. (**C**) Embryonic extracts from control (lane 1), *lrr-1(RNAi)* (lane 2), *cul-2(RNAi)* (lane 3) and *elb-1(RNAi)* (lane 4) embryos were separated by 10% SDS-PAGE and immunoblotted with LRR-1 (top) and tubulin (bottom) antibodies. (**D**) Fluorescent micrograph of an embryo expressing GFP::LRR-1 during pronuclear meeting.

nucleus, but was excluded from chromatin during mitosis (Fig. 2B). We confirmed the nuclear localization of LRR-1 by analysis of a transgenic line expressing a functional GFP::LRR-1 fusion protein (Fig. 2D). Notably, LRR-1 was no longer nuclear in *cul-2(RNAi)* and *elb-1(RNAi)* embryos (7 of 7 and 27/27 embryos, respectively; Fig. 2B) and accumulated in the cytoplasm. However, LRR-1 protein levels remained unchanged under these conditions (Fig. 2C).

We conclude that LRR-1 is a nuclear protein in the germ line and in early embryos, in which its proper localization requires core subunits of the CRL2 complex.

LRR-1 is essential for cell cycle progression in the *C. elegans* germ line

To determine the function of LRR-1, we characterized *tm3543*, a null allele of *lrr-1* (Fig. 3A). Given that *lrr-1* is a maternal-effect gene, homozygous *lrr-1(tm3543)* embryos derived from heterozygous mothers are rescued by the maternal gene product and develop until adulthood. They systematically develop into sterile adults, however, with a protruding vulva. During the course of vulval development, 22 cells are produced in wild-type animals (Sternberg, 2005); by contrast, *lrr-1(tm3543)* mutants produced a reduced number of vulva cells, resulting in a small and asymmetric L4 invagination (n=20). Consequently, following eversion, vulvae from *lrr-1* animals protruded abnormally. These phenotypes were fully rescued by wild-type *lrr-1* transgenes, demonstrating that they were caused by the *lrr-1(tm3543)* mutation (Fig. 3B).

The observation that *lrr-1(tm3543)* animals are sterile and display a protruding vulva suggests that LRR-1 might regulate cell cycle progression in the vulva and in the germ line. Cytological examination of fixed germ lines from *lrr-1(tm3543)* mutant animals revealed a highly disorganized mitotic zone with aberrant nuclei (Fig. 3C, upper panel). The total number of germ cells was severely reduced [48±1 nuclei per gonad arm in *lrr-1* mutants (n=15) versus 740±17 nuclei in heterozygous animals (n=4)], and the nuclei were unevenly distributed. Moreover, the mutant nuclei were almost twice the diameter of control nuclei [7.68±1.34 μm (n=70) versus 4.25±0.66 μm (n=40)].

We next analyzed the cell cycle profile of *lrr-1* mutant germ cells by staining wild-type and *lrr-1(tm3543)* mutant germ lines with propidium iodide and determining the DNA content per germ cell by quantifying the fluorescence (see Materials and methods). Most (>40%) *lrr-1(tm3543)* mutant germ cell nuclei were arrested with a 4N DNA content (Fig. 3D). To corroborate this observation, we analyzed the presence of the G2 marker phospho-Y15 Cdk1, the inactive form of Cdk1 (Norbury et al., 1991; Norbury and

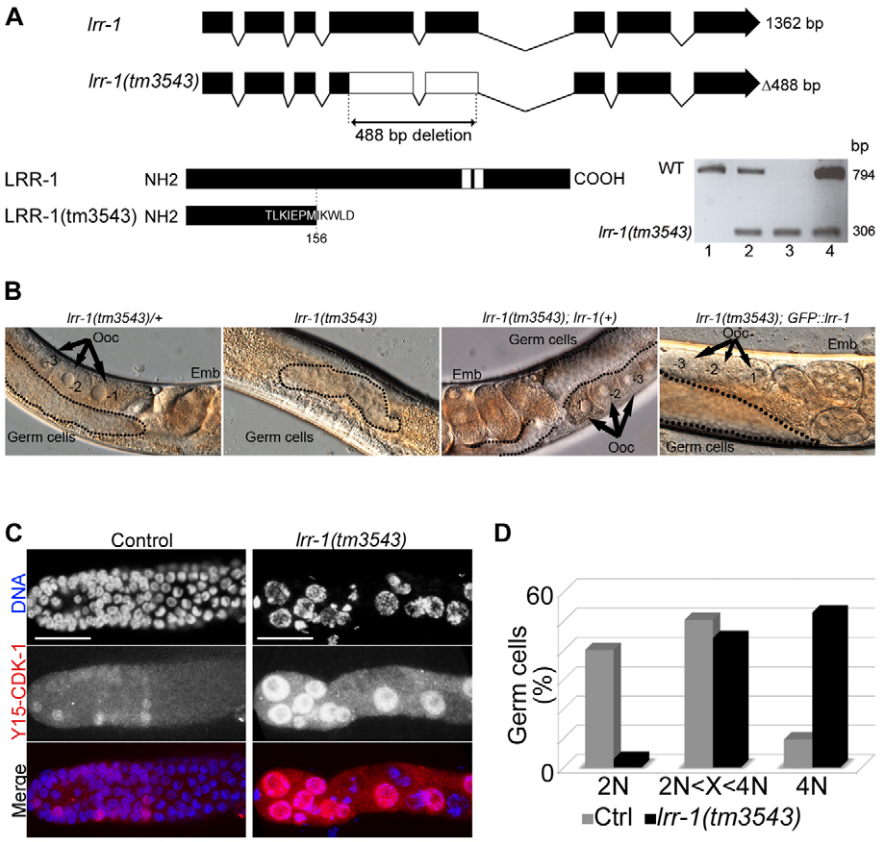

Fig. 3. Loss of *lrr-1* function blocks cell cycle progression in the *C. elegans* germ line, resulting in sterility. (**A**) *lrr-1* gene structure (top) and the predicted protein product (bottom left) for wild-type (WT) N2 animals (453 amino acids) and the *lrr-1(tm3543)* deletion mutant (156 + 6 amino acids, predicted). *lrr-1(tm3543)* carries a 488 bp deletion in the fourth and fifth exons that generates a premature stop codon. (Right) PCR analysis performed with *lrr-1*-specific primers on wild-type (lane 1), heterozygous *lrr-1(tm3543)* (lane 2), homozygous *lrr-1(tm3543)* (lane 3) and homozygous *lrr-1(tm3543)* complemented with the wild-type *lrr-1* gene (lane 4) single worms. (**B**) Micrographs of adult worms of the indicated genotypes analyzed by DIC microscopy. The arrows indicate the position of the oocytes (Ooc) relative to the spermatheca. The germ line is outlined and the presence of embryos (Emb) is indicated. (**C**) Representative images of fixed wild-type and *lrr-1(tm3543)* mutant germ lines (distal part) stained with the Y15-CDK-1 antibody (red) and counterstained with DAPI (blue). Scale bars: 20 μm. (**D**) The percentage of germ cells with a DNA content of 2N, 2N<X<4N and ≥4N in wild-type controls (Ctrl) and *lrr-1(tm3543)* mutants. The quantity of DNA per nucleus was obtained by quantifying the fluorescence of each pixel contained within the volume of the nucleus following propidium iodide staining. *n*=389 and *n*=242 germ cell nuclei in wild type and *lrr-1(tm3543)* mutant, respectively.

Nurse, 1992). As shown in Fig. 3C, most of the germ cell nuclei were stained with the phospho-CDK-1 antibody in the *lrr-1(tm3543)* mutant germ line, as compared with the wild-type situation in which only a few germ cell nuclei were stained. These mutant germ cells were delayed or arrested prior to mitosis, as we did not observe an accumulation of cells positive for the mitotic marker phospho-histone H3 (data not shown).

Collectively, these observations indicate that LRR-1 promotes cell cycle progression through the G2 phase of the cell cycle in the mitotic region of the *C. elegans* germ line.

The ATL-1/CHK-1 checkpoint pathway prevents cell cycle progression in the *lrr-1(tm3543)* mutant germ line

In eukaryotes, the onset of mitosis is controlled by inhibitory phosphorylation of the cell cycle kinase Cdk1 on Y15. This mechanism of mitotic control is also used in the DNA replication checkpoint to prevent mitotic entry in the presence of DNA replication defects or damaged DNA. Stalled replication forks activate the ATR/Chk1 checkpoint pathway, which inactivates Cdc25, the Cdk1 (Y15) phosphatase, thereby preventing cell cycle progression (Harper and Elledge, 2007). To test whether the cell cycle defects observed in the *lrr-1(tm3543)* mutant germ line were dependent on the ATR/Chk1 pathway, we inactivated *atl-1* and *chk-1* in *lrr-1(tm3543)* mutants. Interestingly, *atl-1* and *chk-1* inactivation restored the germ cell proliferation and germ line morphology of *lrr-1(tm3543)* mutants. More strikingly, inactivation of these two genes also restored *lrr-1(tm3543)* mutant fertility (Fig. 4A). The suppression phenotype was highly penetrant, as more than 90% and 60% of *atl-1(RNAi); lrr-1(tm3543)* and *chk-1(RNAi); lrr-1(tm3543)* animals, respectively, were fertile (*n*>100), whereas 100% of *lrr-1(tm3543)* mutants treated with control RNAi were sterile (*n*>100) under the same conditions. Inactivation of *atl-1* similarly suppressed the sterility phenotype of another null allele of *lrr-1*, *ok3435* (data not shown).

To confirm these observations, we constructed a *atl-1(tm853); lrr-1(tm3543)* double mutant. As seen with RNAi, the *atl-1(tm853)* mutation (*tm853* is a null *atl-1* allele) fully suppressed *lrr-1(tm3543)* mutant sterility and the double mutant readily produced non-viable embryos (Fig. 4B, lower panel). Remarkably, *atl-1(RNAi); lrr-1(tm3543)* embryos divided like *atl-1(RNAi); lrr-1(tm3543)/+*; in particular, no signs of severe DNA segregation defects were apparent in these embryos (Fig. 4C). We conclude that the ATL-1/CHK-1 checkpoint pathway prevents cell cycle progression in the *lrr-1* mutant germ line.

The ATL-1/CHK-1 checkpoint pathway delays cell cycle progression in the early embryo upon loss of the CRL2[LRR-1] complex

In the early embryo, the ATL-1/CHK-1 checkpoint pathway is specifically activated to control the timing of division in the P1 blastomere (Brauchle et al., 2003). Thus, if LRR-1 negatively regulates the ATL-1/CHK-1 signaling pathway, its depletion would affect the timing of P1 division, causing embryonic lethality. Consistent with this hypothesis, *lrr-1* was identified in a genome-wide RNAi-based screen combined with video recording of the first embryonic divisions as a gene required for determining the timing of the P lineage division (Sonnichsen et al., 2005). We confirmed these observations and found that downregulation of *lrr-1* by RNAi resulted in a penetrant embryonic lethal phenotype, as more than 95% of the embryos derived from RNAi-treated animals failed to hatch (*n*>200). Time-lapse GFP fluorescence and differential

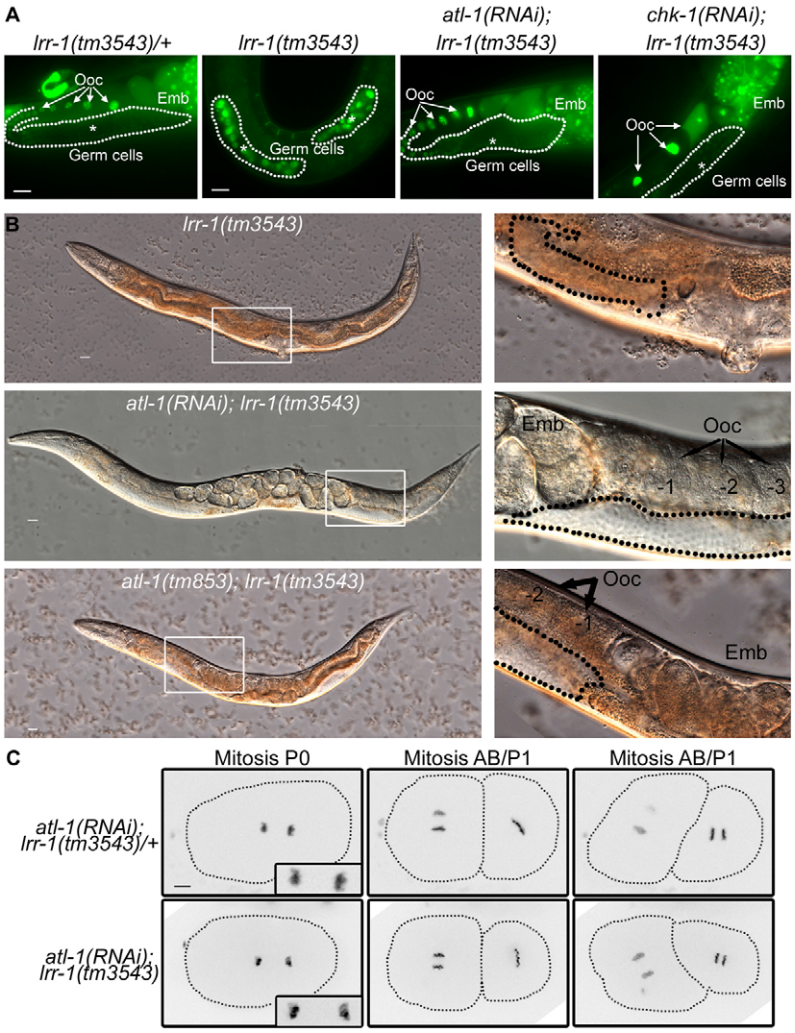

Fig. 4. The DNA replication checkpoint prevents cell cycle progression in *lrr-1(tm3543)* germ cells. (**A**) Fluorescence images of animals of the indicated genotypes carrying the *GFP::H2B* transgene. An asterisk indicates the position of the germ line. (**B**) Micrographs of adult worms of the indicated genotypes analyzed by DIC microscopy. The boxed regions are shown at higher magnification to the right. (**C**) Chromosome segregation during anaphase in P0, AB and P1 blastomeres (outlined) in *lrr-1(tm3543)* heterozygous (top) and homozygous (bottom) mutant embryos lacking *atl-1* function. Representative embryos are shown. Insets illustrate segregating chromosomes at higher magnification. Scale bars: 20 μm in A,B; 5 μm in C.

interference contrast (DIC) microscopy confirmed that the timing of P1 cell division was aberrant in *lrr-1(RNAi)* embryos (Fig. 5A). Whereas in wild-type embryos, there was invariably a 2-minute delay between anaphase onset in the AB and P1 blastomeres (124±3 seconds, *n*=8), this time window reached more than 6 minutes in *lrr-1(RNAi)* embryos (390±59 seconds, *n*=9). Consistent with LRR-1 being part of a CRL2 complex, similar, although more severe, phenotypes were observed upon inactivation of the core CRL2 subunit ELB-1 (1059±59 seconds, *n*=10). The P1 blastomere was delayed prior to mitosis in these embryos as confirmed by the accumulation of phospho-Y15 CDK-1 (Fig. 5B). As anticipated, this delay was dependent on the ATL-1/CHK-1 pathway as it was entirely suppressed in *atl-1(tm853)* mutant embryos (Fig. 5C,D). We also confirmed these observations by evaluating *atl-1(RNAi); lrr-1(tm3543)* embryos expressing histone H2B fused to GFP and similarly observed that *atl-1* was epistatic to *lrr-1(tm3543)* with respect to cell cycle timing: the elapsed time between AB and P1 anaphase was 86±1.02 seconds in *atl-1(RNAi); lrr-1(+/–)* embryos (*n*=11) versus 90±0.79 seconds in *atl-1(RNAi); lrr-1(–/–)* embryos (*n*=20). Taken together, these genetic data indicate that the ATL-1/CHK-1 pathway is activated in early embryos upon inactivation of the $CRL2^{LRR-1}$ complex.

To demonstrate molecular activation of this pathway, we used an antibody that recognizes the activated form of CHK-1 (phospho-S345 CHK-1). Under our conditions, this antibody stained the P granules and centrosomes in wild-type embryos (*n*=40), but this staining was not significantly reduced in *chk-1(RNAi)* or *atl-1(RNAi)* embryos (*n*=59 and *n*=15, respectively). By contrast, nuclear staining was specifically detected in *lrr-1(RNAi)* and *elb-1(RNAi)* embryos (38 of 44 and 41 of 48 embryos, respectively) (Fig. 5E), demonstrating that CHK-1 was specifically activated upon inactivation of the $CRL2^{LRR-1}$ complex. These observations indicate that LRR-1 affects the AB-P1 asynchrony of cell division in the early *C. elegans* embryo by negatively regulating the DNA replication checkpoint. LRR-1 has no impact, however, on the levels or localization of PLK-1 (data not shown) or CDC-25.1 (Fig. 5F), which localize asymmetrically between the AB and P1 blastomeres and regulate the AB-P1 asynchrony of cell division (Budirahardja and Gonczy, 2008; Rivers et al., 2008).

ssDNA-RPA-1 nuclear foci activate the DNA replication checkpoint in *lrr-1* mutants

Why is the ATL-1/CHK-1 checkpoint pathway hyperactivated upon *lrr-1* inactivation? Checkpoint activation may arise from defects in DNA replication and its integrity, or, alternatively, the checkpoint might be constitutively activated independently of DNA replication defects. The finding that ATL-1/CHK-1 pathway inactivation readily suppressed *lrr-1(tm3543)* mutant sterility suggests that this pathway is not activated as a consequence of severe DNA replication defects. Indeed, if the checkpoint were

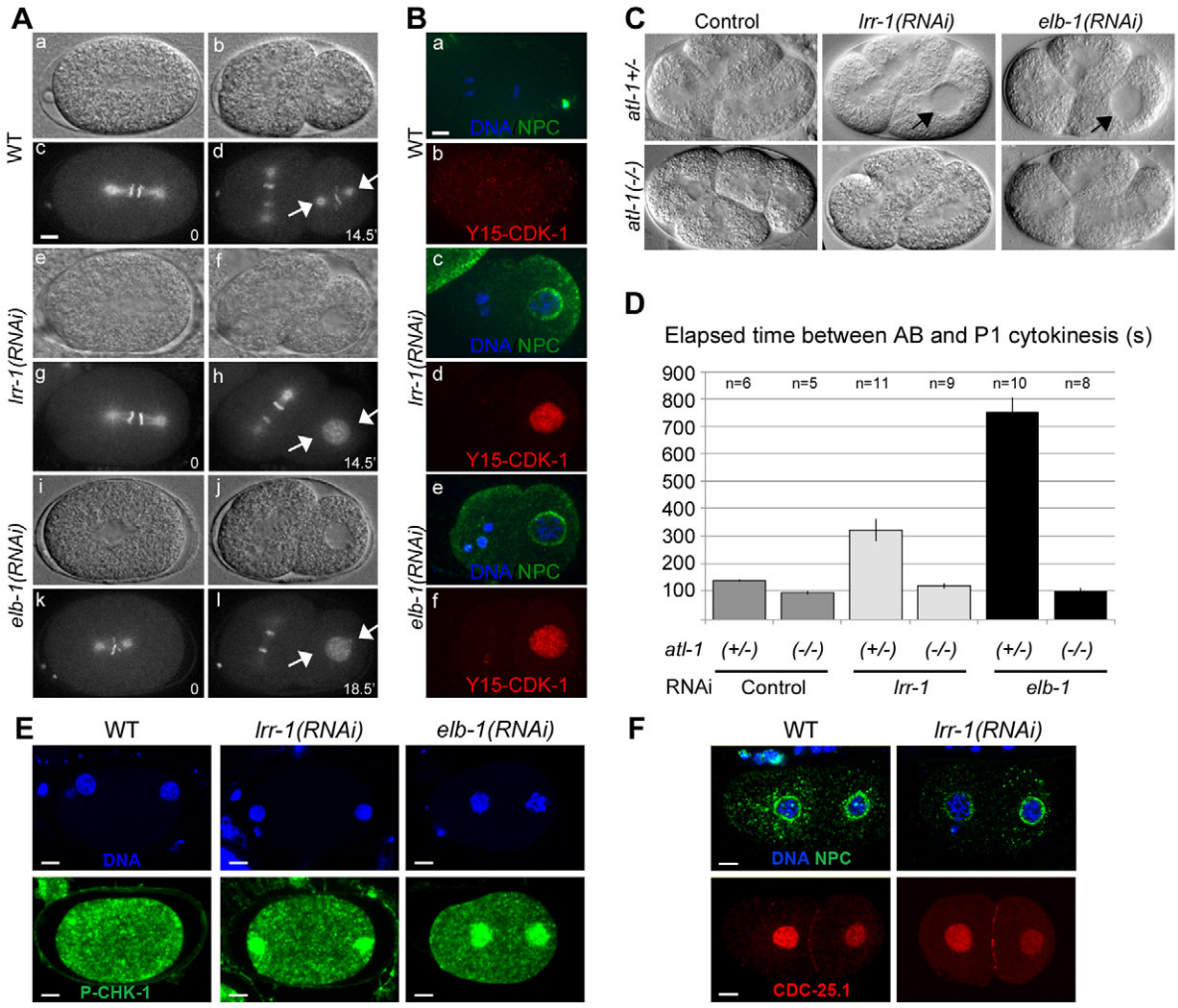

Fig. 5. The DNA replication checkpoint delays cell cycle progression in early *C. elegans* embryos. (**A**) DIC and GFP fluorescence micrographs of (**a-d**) wild-type, (**e-h**) *lrr-1(RNAi)* and (**i-l**) *elb-1(RNAi)* embryos expressing histone H2B and tubulin fused to GFP during metaphase or anaphase of the first and second division. Arrows mark the position of centrosomes in the P1 blastomere. (**B**) Representative images of fixed (**a**,**b**) wild-type, (**c**,**d**) *lrr-1(RNAi)* and (**e**,**f**) *elb-1(RNAi)* embryos stained with nucleoporin/Mab414 (green) and phospho-Y15 CDK-1 (red) antibodies and counterstained with DAPI (blue). (**C**) DIC micrographs of heterozygous (+/–) and homozygous (–/–) *atl-1(tm853)* embryos treated with control, *lrr-1* or *elb-1* double-stranded (ds) RNA during the second division. Note the persistence of three-cell stage embryos in the *atl-1(tm853)* heterozygous mutant that were treated with *lrr-1* or *elb-1* dsRNA. Arrowheads mark intact nuclei. (**D**) The elapsed time (s, seconds) between AB and P1 cytokinesis in heterozygous (+/–) and homozygous (–/–) *atl-1(tm853)* mutant embryos treated with non-specific (dark gray), *lrr-1* (gray) or *elb-1* (black) dsRNA. Error bars indicate s.e.m.; *n*, the number of embryos analyzed of the indicated genotypes. (**E**) Fixed wild-type, *lrr-1(RNAi)* and *elb-1(RNAi)* embryos stained with a phospho-S345 CHK-1 antibody (green) and counterstained with DAPI (blue). (**F**) Fixed wild-type and *lrr-1(RNAi)* embryos stained with nucleoporin/Mab414 (green) and CDC-25.1 (red) antibodies and counterstained with DAPI (blue). Scale bars: 5 μm.

activated as a consequence of hampered DNA replication, the *lrr-1(tm3543); atl-1(tm853)* double mutants would be sterile owing to the persistence of DNA replication defects. Consistent with this prediction, RNAi-mediated inactivation of *atl-1* exacerbated the sterility phenotype of the DNA replication mutant *div-1(or148)*, which exhibits inefficient priming of Okazaki fragments (Encalada et al., 2000) (Fig. 6A). Likewise, *atl-1(tm853)* larvae exposed to low concentrations of hydroxyurea (HU), which induces stalled replication forks by depleting the pool of dNTPs, readily developed into sterile animals, whereas wild-type N2 animals were eightfold more resistant to HU-induced sterility at 8 mM HU (Fig. 6B).

Although these observations suggest that the DNA replication checkpoint is not activated as a consequence of severe DNA replication defects, they do not exclude the possibility that some forms of DNA damage accumulate in the *lrr-1* mutants that activate the DNA replication checkpoint. To further investigate this possibility, we analyzed the formation of replication protein A (RPA-1) nuclear foci in *lrr-1* mutant germ cells using a specific antibody (Lee et al., 2010). RPA-1 binds single-stranded (ss) DNA, and ssDNA-RPA-1 complexes contribute to the recruitment and activation of ATL-1 at sites of DNA damage (Garcia-Muse and Boulton, 2005). Unlike wild-type worms, *lrr-1* mutants exhibited stretches of ssDNA, as evidenced by the accumulation of RPA-1 nuclear foci, and this phenotype was even more pronounced in *atl-1(RNAi); lrr-1(tm3543)* animals (Fig. 6C). Taken together, these observations indicate that a form of DNA damage accumulates in *lrr-1* mutants and activates the DNA replication checkpoint.

To determine the origin of this DNA damage, we analyzed the cell cycle profile of *atl-1(RNAi); lrr-1(tm3543)* germ cell nuclei after propidium iodide staining, as described previously in Fig. 3D.

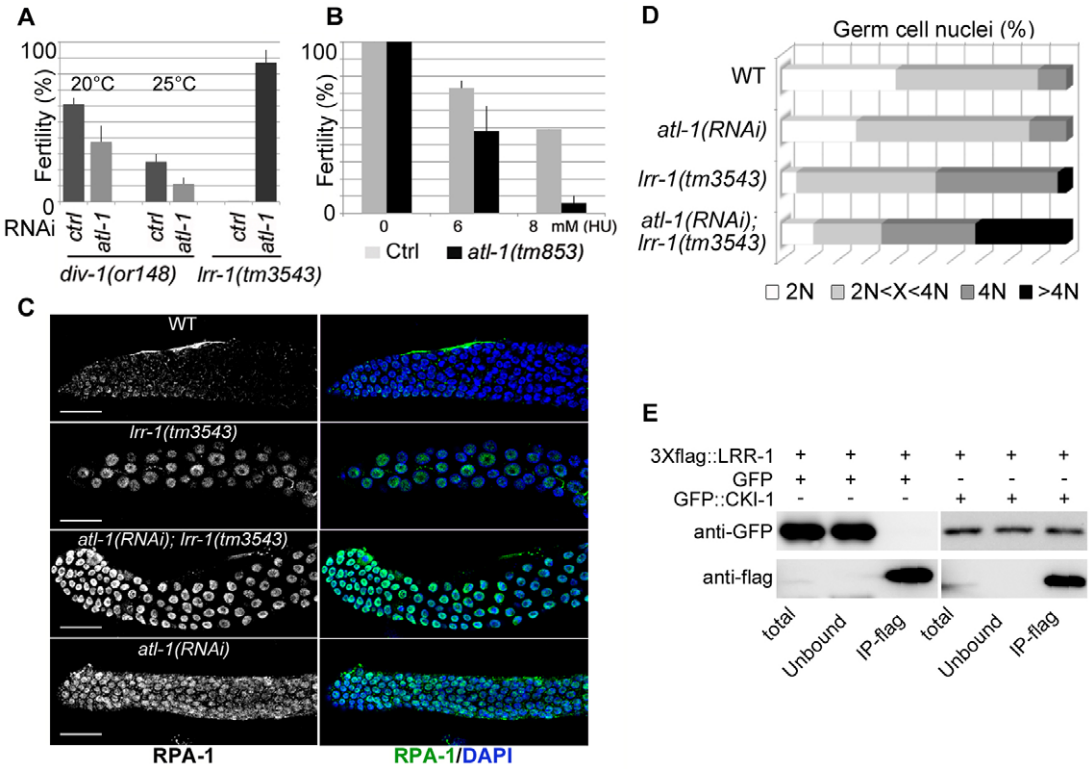

Fig. 6. LRR-1 controls DNA replication integrity. (**A**) The percentage of fertile animals of the indicated genotypes after a control treatment or RNAi inactivation of *atl-1*. The results are representative of three independent experiments. (**B**) The percentage of fertile wild-type and *atl-1(tm853)* animals upon exposure to 6 and 8 mM hydroxyurea (HU). Error bars in A and B represent ± s.d. (**C**) Representative images of mitotic germ lines of the indicated genotypes stained with an RPA-1 antibody (green) and counterstained with DAPI (blue). Scale bars: 20 μm. (**D**) The percentage of germ cell nuclei of the indicated genotypes with a DNA content of 2N (white), between 2N and 4N (gray), 4N (dark gray) and greater than 4N (black). Wild type, *n*=389; *atl-1(RNAi)*, *n*=923; *lrr-1(tm3543)*, *n*=251; and *atl-1(RNAi); lrr-1(tm3543)*, *n*=691 nuclei. (**E**) FLAG::LRR-1 immunoprecipitates from HEK293T cells expressing GFP or GFP::CKI-1 were immunoblotted with specific GFP (top) and FLAG (bottom) antibodies.

Remarkably, this analysis revealed that a large proportion of germ cells (30%) showed a DNA content greater than 4N in *atl-1(RNAi); lrr-1(tm3543)* mutants (Fig. 6D), suggesting that some regions of the genome might have undergone DNA re-replication under these conditions. Notably, this analysis also showed that a small percentage of germ cell nuclei (<2%) showed a DNA content greater than 4N in the single *lrr-1(tm3543)* mutant, whereas this phenotype was never observed in wild-type or *atl-1(RNAi)* animals (Fig. 6D).

Taken together, these observations suggest that LRR-1 is required to suppress re-replication. The underlying molecular mechanisms, however, are currently unclear. Interestingly, CUL-2 has been previously implicated in the degradation of the CDK inhibitor CKI-1 (Feng et al., 1999), and it has been shown, at least in mitotic cells, that CKI-1 accumulation in S phase contributes to the re-replication phenotype (Kim et al., 2008). Therefore, we investigated whether LRR-1 might be involved in CKI-1 degradation. Although we could detect a specific physical interaction between LRR-1 and CKI-1 in a heterologous human HEK293T cell system (Fig. 6E), *cki-1* depletion by RNAi (feeding, soaking or injection) failed to suppress cell cycle arrest in *C. elegans lrr-1* germ cells, suggesting that CKI-1 might not be the only LRR-1 target. Nevertheless, CKI-1 accumulation might contribute to the observed re-replication phenotype.

DISCUSSION

We have identified the leucine-rich repeat protein LRR-1 in *C. elegans* and shown that it functions as a substrate-recruitment subunit of a Cullin 2-based E3 ligase with an essential role in cell cycle progression. *lrr-1(tm3543)* homozygous mutants develop into sterile adults with a small germ line. This severe reduction in germ cell number is due to a failure in germ cell proliferation. Consistent with a proliferation defect, we observed cell cycle arrest in G2 phase in these mutants due to hyperactivation of the DNA replication checkpoint, as this phenotype was entirely suppressed by inactivation of the DNA replication checkpoint genes *atl-1* and *chk-1*. Importantly, inactivation of these genes not only released the cell cycle block, but also rescued fertility of the *lrr-1(tm3543)* mutants, suggesting that LRR-1 is required for mitotic proliferation of the germ line but is dispensable for meiosis. Similar to the situation in germ cells, RNAi inactivation of *lrr-1* in early embryos led to hyperactivation of the DNA replication checkpoint, causing a cell cycle delay in the division of the P lineage and resulting in embryonic lethality. Hyperactivation of this checkpoint is not constitutive in *lrr-1* mutants, but is likely to be a consequence of the accumulation of stretches of ssDNA, which may arise due to DNA re-replication (Fig. 7). Collectively, our observations identify the $CRL2^{LRR-1}$ complex as an important determinant of replication integrity and genome stability in *C. elegans*.

Identification of a Cullin 2-based E3 ligase containing the LRR-1 protein in *C. elegans*

The LRR-1 protein is evolutionarily conserved, but its function remains elusive. Protein sequence analysis revealed that LRR-1 contains a typical BC/Cul-2 box at its C-terminus and binds other CRL2 subunits both in vitro and in vivo in a BC/Cul-2 box-

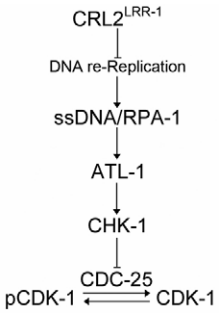

Fig. 7. Model for CRL2^{LRR-1} function. Loss of *lrr-1* function induces re-replication and causes the accumulation of stretches of ssDNA. ssDNA-RPA-1 nuclear foci then recruit and activate ATL-1, which, together with the CHK-1 kinase, prevents CDK-1 activation (dephosphorylation via CDC-25) and cell cycle progression.

dependent manner. Notably, LRR-1 is unlikely to be able to adopt its native conformation in the absence of the CRL2 core subunits ELB-1 and ELC-1. Indeed, LRR-1 was insoluble in bacteria but was recovered in a soluble, stable, trimeric complex when it was co-expressed with ELB-1 and ELC-1. This property is reminiscent of the tumor suppressor VHL (Von Hippel-Lindau), which targets the transcription factor hypoxia-inducible factor 1 (HIF1) for proteasomal degradation and, like LRR-1, requires ELB1 and ELC1 in order to adopt its native conformation (Stebbins et al., 1999; Sutovsky and Gazit, 2004). Importantly, the VHL binding site for HIF1/2α is only formed in the presence of ELB1 and ELC1 (Hon et al., 2002; Min et al., 2002). Since LRR-1 was mislocalized in *cul-2* and *elb-1(RNAi)* embryos, it is tempting to speculate that LRR-1 similarly requires CRL2 components to fold and properly engage its substrates.

Hyperactivation of the DNA replication checkpoint upon loss of the CRL2^{LRR-1} complex

Phenotypic analysis of *lrr-1(tm3543)* mutants and *lrr-1(RNAi)* embryos revealed that the DNA replication checkpoint was hyperactivated in the absence of LRR-1. Activation of this checkpoint culminates in the recruitment and activation of ATR kinase at sites of DNA damage or stalled replication forks (Cimprich and Cortez, 2008; Segurado and Tercero, 2009; Zegerman and Diffley, 2009). When DNA polymerases stall, the replicative minichromosome maintenance (MCM) helicases continue to unwind the DNA ahead of the fork, generating ssDNA (Byun et al., 2005), which is subsequently coated by the ssDNA-binding protein RPA-1. Along with other factors, ssDNA-RPA-1 complexes contribute to the recruitment and activation of ATR at sites of DNA damage. Once activated, ATR phosphorylates Chk1, which in turn blocks cell cycle progression by inhibiting the Cdc25 phosphatase. Here, we provide compelling evidence that the DNA replication checkpoint is activated upon loss of *lrr-1* function: CHK-1 was found to be specifically phosphorylated at the ATR/ATL-1 phosphorylation site (S345) in *lrr-1(RNAi)* embryos, and ssDNA-RPA-1 nuclear foci accumulated in *lrr-1* germ cells.

However, we did not detect massive DNA damage or replication failure in *lrr-1* mutants. For example, RAD-51 nuclear foci, which are indicative of fork collapse, were not detected in *lrr-1* mutants (0.06% of germ cells had RAD-51 nuclear foci, n=86), whereas they readily accumulated in *atl-1(tm853)* germ cells (58%, n=113). Moreover, despite the appearance of ssDNA stretches, *lrr-1* mutants did not show the classical phenotypes of DNA replication mutants. For example, DNA segregation is often impaired when DNA replication is compromised (Mouysset et al., 2008) and this phenotype is exacerbated in the absence of a functional DNA replication checkpoint (Brauchle et al., 2003). Massive DNA segregation defects were not apparent in *lrr-1(tm3543)* or *atl-1(RNAi); lrr-1(tm3543)* embryos, although some minor DNA bridges were detected by spinning-disk microscopy in the latter case (data not shown). Furthermore, whereas the ATL-1/CHK-1 checkpoint pathway is essential for animal fertility when DNA replication is challenged, it appears to be dispensable in *lrr-1* mutants given that *lrr-1; atl-1* double-mutant animals were fully fertile.

These observations suggest that although DNA damage is relatively minor in *lrr-1* mutants, it is sufficient to trigger a checkpoint response, which is consistent with recent data indicating that a stretch of 200-1000 nucleotides is sufficient to trigger a robust checkpoint response, at least in vitro (Choi et al., 2010).

The CRL2^{LRR-1} complex and the integrity of DNA replication

The origin of the DNA damage that occurs in *lrr-1* mutants is currently unclear, as ssDNA-RPA-1 is a structural intermediate common to several DNA metabolic processes. Given that *atl-1(RNAi); lrr-1* mutant germ cells accumulated with a DNA content greater than 4N, it is tempting to speculate that some regions of the genome might have undergone re-replication. DNA replication is a complex task that involves the activation of a large number of replication origins distributed throughout the chromatin. Strict temporal regulation of DNA replication and its separation in two distinct steps ensure that DNA is replicated only once per cell cycle (Blow and Dutta, 2005; Arias and Walter, 2007). These two steps are regulated by the periodic oscillation of CDK activity during the cell cycle. In a first step, which takes place at the end of mitosis and during early G1, when CDK activity is low, pre-replicative complexes (pre-RCs) assemble on replication origins. In a second step, during S phase, CDKs and DDKs (Dbf4-dependent kinases) activate the MCM replicative helicase (Labib, 2010).

During S phase, the assembly of new pre-RCs must be prevented and several mechanisms contribute to pre-RC inactivation, including Cdt1 degradation and Cdc6 nuclear export (Arias and Walter, 2007). In *C. elegans*, the CRL4^{Cdt2} complex is instrumental for pre-RC disassembly by promoting the degradation of the licensing factor CDT-1 (Zhong et al., 2003) and facilitating CDC-6 nuclear export via degradation of the CDK inhibitor CKI-1 (Kim et al., 2008). Interestingly, CUL-2 has been implicated in the degradation of CKI-1 in the germ line (Feng et al., 1999) and LRR-1 physically interacts with CKI-1, suggesting that CKI-1 is an LRR-1 target. *cki-1* depletion by RNAi, however, failed to suppress cell cycle arrest in *lrr-1* germ cells, suggesting that CKI-1 might not be the only target of LRR-1. Consistent with this prediction, CKI-1 levels are unchanged in *cul-2(ek1)* mutant embryos (Feng et al., 1999). Nevertheless, CKI-1 might contribute to the observed phenotype. Further characterization of the CRL2^{LRR-1} complex and identification of its critical target(s) will certainly shed light on this important new mechanism in the maintenance of genome integrity during DNA replication.

Acknowledgements

We thank S. Tan, S. Mitani, E. Kipreos, J. Reboul, P. Gonczy, the Caenorhabditis Genetics Center (funded by the NIH Center for Research Resources), R. Sonneville, I. Johnstone, A. Gartner, H. S. Koo and S. Boulton for strains and reagents; M. Peter for support; M. Tyers (in whose laboratory this work was initiated) and all members of the Institut Jacques Monod Imaging facility (ImagoSeine) for their assistance; and M. A. Félix for generously sharing

equipment. J.B. is supported by a PhD fellowship from the French Ministry of Education and Research and J.M. by a CNRS and La Ligue Contre le Cancer fellowship. Work in the L.P. laboratory is supported by an ATIP grant from the CNRS, the Association pour la Recherche sur le Cancer (ARC), the Fondation pour la Recherche Médicale (FRM) and the City of Paris.

Competing interests statement

The authors declare no competing financial interests.

References

Arias, E. E. and Walter, J. C. (2007). Strength in numbers: preventing rereplication via multiple mechanisms in eukaryotic cells. *Genes Dev.* **21**, 497-518.
Blow, J. J. and Dutta, A. (2005). Preventing re-replication of chromosomal DNA. *Nat. Rev. Mol. Cell Biol.* **6**, 476-486.
Brauchle, M., Baumer, K. and Gonczy, P. (2003). Differential activation of the DNA replication checkpoint contributes to asynchrony of cell division in C. elegans embryos. *Curr. Biol.* **13**, 819-827.
Brenner, S. (1974). The genetics of Caenorhabditis elegans. *Genetics* **77**, 71-94.
Budirahardja, Y. and Gonczy, P. (2008). PLK-1 asymmetry contributes to asynchronous cell division of C. elegans embryos. *Development* **135**, 1303-1313.
Byun, T. S., Pacek, M., Yee, M. C., Walter, J. C. and Cimprich, K. A. (2005). Functional uncoupling of MCM helicase and DNA polymerase activities activates the ATR-dependent checkpoint. *Genes Dev.* **19**, 1040-1052.
Choi, J. H., Lindsey-Boltz, L. A., Kemp, M., Mason, A. C., Wold, M. S. and Sancar, A. (2010). From the cover: reconstitution of RPA-covered single-stranded DNA-activated ATR-Chk1 signaling. *Proc. Natl. Acad. Sci. USA* **107**, 13660-13665.
Cimprich, K. A. and Cortez, D. (2008). ATR: an essential regulator of genome integrity. *Nat. Rev. Mol. Cell Biol.* **9**, 616-627.
Edgley, M. L. and Riddle, D. L. (2001). LG II balancer chromosomes in Caenorhabditis elegans: mT1(II;III) and the mIn1 set of dominantly and recessively marked inversions. *Mol. Genet. Genomics* **266**, 385-395.
Encalada, S. E., Martin, P. R., Phillips, J. B., Lyczak, R., Hamill, D. R., Swan, K. A. and Bowerman, B. (2000). DNA replication defects delay cell division and disrupt cell polarity in early Caenorhabditis elegans embryos. *Dev. Biol.* **228**, 225-238.
Feng, H., Zhong, W., Punkosdy, G., Gu, S., Zhou, L., Seabolt, E. K. and Kipreos, E. T. (1999). CUL-2 is required for the G1-to-S-phase transition and mitotic chromosome condensation in *Caenorhabditis elegans*. *Nat. Cell Biol.* **1**, 486-492.
Flicek, P., Aken, B. L., Ballester, B., Beal, K., Bragin, E., Brent, S., Chen, Y., Clapham, P., Coates, G., Fairley, S. et al. (2010). Ensembl's 10th year. *Nucleic Acids Res.* **38**, D557-D562.
Garcia-Muse, T. and Boulton, S. J. (2005). Distinct modes of ATR activation after replication stress and DNA double-strand breaks in Caenorhabditis elegans. *EMBO J.* **24**, 4345-4355.
Gartner, A., Milstein, S., Ahmed, S., Hodgkin, J. and Hengartner, M. O. (2000). A conserved checkpoint pathway mediates DNA damage – induced apoptosis and cell cycle arrest in C. elegans. *Mol. Cell* **5**, 435-443.
Harper, J. W. and Elledge, S. J. (2007). The DNA damage response: ten years after. *Mol. Cell* **28**, 739-745.
Holway, A. H., Kim, S. H., La Volpe, A. and Michael, W. M. (2006). Checkpoint silencing during the DNA damage response in Caenorhabditis elegans embryos. *J. Cell Biol.* **172**, 999-1008.
Hon, W. C., Wilson, M. I., Harlos, K., Claridge, T. D., Schofield, C. J., Pugh, C. W., Maxwell, P. H., Ratcliffe, P. J., Stuart, D. I. and Jones, E. Y. (2002). Structural basis for the recognition of hydroxyproline in HIF-1 alpha by pVHL. *Nature* **417**, 975-978.
Kalogeropoulos, N., Christoforou, C., Green, A. J., Gill, S. and Ashcroft, N. R. (2004). chk-1 is an essential gene and is required for an S-M checkpoint during early embryogenesis. *Cell Cycle* **3**, 1196-1200.
Kamath, R. S., Martinez-Campos, M., Zipperlen, P., Fraser, A. G. and Ahringer, J. (2001). Effectiveness of specific RNA-mediated interference through ingested double-stranded RNA in Caenorhabditis elegans. *Genome Biol.* **2**, RESEARCH0002.
Kamura, T., Maenaka, K., Kotoshiba, S., Matsumoto, M., Kohda, D., Conaway, R. C., Conaway, J. W. and Nakayama, K. I. (2004). VHL-box and SOCS-box domains determine binding specificity for Cul2-Rbx1 and Cul5-Rbx2 modules of ubiquitin ligases. *Genes Dev.* **18**, 3055-3065.
Kim, Y., Starostina, N. G. and Kipreos, E. T. (2008). The CRL4Cdt2 ubiquitin ligase targets the degradation of p21Cip1 to control replication licensing. *Genes Dev.* **22**, 2507-2519.
Kimble, J. E. and White, J. G. (1981). On the control of germ cell development in Caenorhabditis elegans. *Dev. Biol.* **81**, 208-219.
Kimble, J. and Crittenden, S. L. (2007). Controls of germline stem cells, entry into meiosis, and the sperm/oocyte decision in Caenorhabditis elegans. *Annu. Rev. Cell Dev. Biol.* **23**, 405-433.
Labib, K. (2010). How do Cdc7 and cyclin-dependent kinases trigger the initiation of chromosome replication in eukaryotic cells? *Genes Dev.* **24**, 1208-1219.
Lee, S. J., Gartner, A., Hyun, M., Ahn, B. and Koo, H. S. (2010). The Caenorhabditis elegans Werner syndrome protein functions upstream of ATR and ATM in response to DNA replication inhibition and double-strand DNA breaks. *PLoS Genet.* **6**, 1000801.
Luke-Glaser, S., Roy, M., Larsen, B., Le Bihan, T., Metalnikov, P., Tyers, M., Peter, M. and Pintard, L. (2007). CIF-1, a shared subunit of the COP9/signalosome and eukaryotic initiation factor 3 complexes, regulates MEL-26 levels in the Caenorhabditis elegans embryo. *Mol. Cell. Biol.* **27**, 4526-4540.
Mahrour, N., Redwine, W. B., Florens, L., Swanson, S. K., Martin-Brown, S., Bradford, W. D., Staehling-Hampton, K., Washburn, M. P., Conaway, R. C. and Conaway, J. W. (2008). Characterization of Cullin-box sequences that direct recruitment of Cul2-Rbx1 and Cul5-Rbx2 modules to Elongin BC-based ubiquitin ligases. *J. Biol. Chem.* **283**, 8005-8013.
Mello, C. C., Kramer, J. M., Stinchcomb, D. and Ambros, V. (1991). Efficient gene transfer in C. elegans: extrachromosomal maintenance and integration of transforming sequences. *EMBO J.* **10**, 3959-3970.
Min, J. H., Yang, H., Ivan, M., Gertler, F., Kaelin, W. G., Jr and Pavletich, N. P. (2002). Structure of an HIF-1a-pVHL complex: hydroxyproline recognition in signaling. *Science* **296**, 1886-1889.
Moser, S. C., von Elsner, S., Bussing, I., Alpi, A., Schnabel, R. and Gartner, A. (2009). Functional dissection of Caenorhabditis elegans CLK-2/TEL2 cell cycle defects during embryogenesis and germline development. *PLoS Genet.* **5**, e1000451.
Mouysset, J., Deichsel, A., Moser, S., Hoege, C., Hyman, A. A., Gartner, A. and Hoppe, T. (2008). Cell cycle progression requires the CDC-48UFD-1/NPL-4 complex for efficient DNA replication. *Proc. Natl. Acad. Sci. USA* **105**, 12879-12884.
Norbury, C. and Nurse, P. (1992). Animal cell cycles and their control. *Annu. Rev. Biochem.* **61**, 441-470.
Norbury, C., Blow, J. and Nurse, P. (1991). Regulatory phosphorylation of the p34cdc2 protein kinase in vertebrates. *EMBO J.* **10**, 3321-3329.
Olma, M. H., Roy, M., Le Bihan, T., Sumara, I., Maerki, S., Larsen, B., Quadroni, M., Peter, M., Tyers, M. and Pintard, L. (2009). An interaction network of the mammalian COP9 signalosome identifies Dda1 as a core subunit of multiple Cul4-based E3 ligases. *J. Cell Sci.* **122**, 1035-1044.
Paulsen, R. D. and Cimprich, K. A. (2007). The ATR pathway: fine-tuning the fork. *DNA Rep.* **6**, 953-966.
Petroski, M. D. and Deshaies, R. J. (2005). Function and regulation of cullin-RING ubiquitin ligases. *Nat. Rev. Mol. Cell Biol.* **6**, 9-20.
Pintard, L., Kurz, T., Glaser, S., Willis, J. H., Peter, M. and Bowerman, B. (2003). Neddylation and deneddylation of CUL-3 is required to target MEI-1/katanin for degradation at the meiosis-to-mitosis transition in *C. elegans*. *Curr. Biol.* **13**, 911-921.
Reinke, V., Smith, H. E., Nance, J., Wang, J., Van Doren, C., Begley, R., Jones, S. J., Davis, E. B., Scherer, S., Ward, S. et al. (2000). A global profile of germline gene expression in C. elegans. *Mol. Cell* **6**, 605-616.
Rivers, D. M., Moreno, S., Abraham, M. and Ahringer, J. (2008). PAR proteins direct asymmetry of the cell cycle regulators Polo-like kinase and Cdc25. *J. Cell Biol.* **180**, 877-885.
Sambrook, J., Fristch, E. F. and Maniatis, T. (1989). *Molecular Cloning: A Laboratory Manual*, 2nd edn. Cold Spring harbor, NY: Cold Spring Harbor Laboratory Press.
Segref, A., Cabello, J., Clucas, C., Schnabel, R. and Johnstone, I. L. (2010). Fate specification and tissue-specific cell cycle control of the Caenorhabditis elegans intestine. *Mol. Biol. Cell* **21**, 725-738.
Segurado, M. and Tercero, J. A. (2009). The S-phase checkpoint: targeting the replication fork. *Biol. Cell* **101**, 617-627.
Sonnichsen, B., Koski, L. B., Walsh, A., Marschall, P., Neumann, B., Brehm, M., Alleaume, A. M., Artelt, J., Bettencourt, P., Cassin, E. et al. (2005). Full-genome RNAi profiling of early embryogenesis in Caenorhabditis elegans. *Nature* **434**, 462-469.
Stebbins, C. E., Kaelin, W. G., Jr and Pavletich, N. P. (1999). Structure of the VHL-ElonginC-ElonginB complex: implications for VHL tumor suppressor function. *Science* **284**, 455-461.
Sternberg, P. W. (2005). Vulval development. *WormBook* 1-28. http://www.wormbook.org.
Sutovsky, H. and Gazit, E. (2004). The von Hippel-Lindau tumor suppressor protein is a molten globule under native conditions: implications for its physiological activities. *J. Biol. Chem.* **279**, 17190-17196.
Tan, S. (2001). A modular polycistronic expression system for overexpressing protein complexes in Escherichia coli. *Protein Expr. Purif.* **21**, 224-234.
Vasudevan, S., Starostina, N. G. and Kipreos, E. T. (2007). The Caenorhabditis elegans cell-cycle regulator ZYG-11 defines a conserved family of CUL-2 complex components. *EMBO Rep.* **8**, 279-286.
Zegerman, P. and Diffley, J. F. (2009). DNA replication as a target of the DNA damage checkpoint. *DNA Rep.* **8**, 1077-1088.
Zhong, W., Feng, H., Santiago, F. E. and Kipreos, E. T. (2003). CUL-4 ubiquitin ligase maintains genome stability by restraining DNA-replication licensing. *Nature* **423**, 885-889.